JOURNAL OF MATERIALS SCIENCE **40** (2005) 3325–3337

Wall slip phenomena in talc-filled polypropylene compounds

B. HAWORTH*, S. W. KHAN
Institute of Polymer Technology & Materials Engineering (IPTME), Loughborough University, Loughborough LE11 3TU, UK
E-mail: B.Haworth@lboro.ac.uk

Slip velocities of unfilled and talc-filled polypropylene (PP) compounds, detectable at the die wall during pressure driven shear flow, have been determined using capillary rheometry. The presence of low molar mass, polar additives is responsible for the detection of wall slip in unmodified PP. Slip velocity increases with shear stress, beyond the critical onset condition. Increasing talc concentration in the PP compounds reduces slip velocity systematically, according to the talc volume fraction, whilst talc particle morphology appears to modify the wall slip behaviour to a greater extent than particle size. In comparison to PP-talc composites based on untreated filler, the presence of surface coatings tends to increase wall slip velocity, at any given shear stress, when the coating concentration exceeds monolayer level. These observations are explained in terms of a mechanism for wall slip in a low cohesive strength interphase, rich in low molar mass amide species, close to the flow boundary. This behaviour has also been modelled using a power law, to define wall slip parameters as a function of shear stress and talc concentration that can be used to enhance process simulation. It is demonstrated that the onset and magnitude of wall slip may be controllable by compound formulation and process conditions, creating exploitation potential to enhance process control and product properties of particle-modified PP composites.
© *2005 Springer Science + Business Media, Inc.*

1. Introduction

Incorporation of particulate additives into polymer compounds is now carried out extensively, due to the improvements in a number of functional properties [1, 2]. Moreover, interfacial particle-polymer interactions can be modified using additives such as inert coatings, to enhance dispersion effects, whereas chemical reaction with the polymer can be achieved by using coupling agents, so that interfacial adhesion can be enhanced. However, high concentrations of particulate additives can have significant effects on shear viscosity [3, 4], thereby increasing the required mould-filling pressures in high-speed processes such as injection moulding. The technical driving force for the development of multiphase polymer systems containing particulate additives is their influence on solid-state properties, such as modulus, yield stress and high temperature creep resistance. However, it is also essential to characterise rheological properties that control the processing stage and subsequently influence microstructure development, including pressure driven shear flow and wall slip behaviour.

The latter effect is particularly important in polymer processing, since a condition of zero flow velocity at a constrained flow boundary is a fundamental assumption on which conventional laminar shear flow theory is based [4]. This carries specific relevance to flow analysis and predictive models used to simulate commercial processes, since wall slip effects will influence the accuracy and applicability of the raw data used in flow simulation procedures. Effects on single screw extrusion processes were first analysed by Worth *et al.* [5] and more recent research has considered the influence of wall slipping materials on the extrusion of non-Newtonian materials using 1-dimensional and isothermal flow simulation [6]. The computations were based upon dimensionless quantities of critical shear stress (τ_c^*), wall shear stress (τ_w^*) and velocity difference between wall and melt (v_{sl}^*), which are related by:

$$\tau_w^* = \tau_c^* + k v_{sl}^* \tag{1}$$

where material constant $k = \tau_c^*/a \cdot b$ and parameters a and b are functions of known chemical constants [6,7]. The simulations require appropriate values for parameters τ_c^* and k, alongside material flow properties K (consistency index), n (power law index) and screw design variables, such that the conditions for

*Author to whom all correspondence should be addressed.

wall slippage at both barrel and screw surfaces can be predicted.

Flow instabilities arising from wall slip in high polyolefins have been shown to be sensitive to molecular parameters of the raw material (molar mass and short-chain branching in PE) and process temperature [8]. In contrast to earlier work reported by Ramamurthy [9], the metallic materials from which the capillary dies were constructed also have an influence on the magnitude of wall slip velocity. Similar conclusions have been made from experiments on polyolefins carried out in dies modified by fluoropolymer coatings [10, 11]. The existence of a critical shear stress condition at which finite flow velocity first becomes evident at the polymer-metal interface is highly significant and has been recognised previously [6, 7, 10, 12]. Furthermore, it has been proposed that this parameter correlates with the work of adhesion at the flow boundary surfaces [13], a hypothesis that has been subsequently verified by experimental data [10], suggesting that the assumption that slip occurs as a result of adhesive failure may be correct.

If the mechanism of slip is to be established in any given situation, it should be determined whether wall slip occurs by adhesive failure at the die/mould wall, or whether cohesive failure occurs within the polymer melt, at a position close to the flow boundary. The presence of particulate additives, whether unmodified or if chemically treated, will potentially influence each of these outcomes. Previous research has established that wall slip in PP-$CaCO_3$ compounds may occur, or be exacerbated by the presence of dispersion-promoting coatings such as fatty acids [14]. In contrast, uncoated magnesium hydroxide flame retardant has been shown to be responsible for wall slip in MDPE, an effect negated when stearic acid coatings were applied [15]. Also, there are many published examples of wall slip effects occurring in unfilled polymers, notably when analysed under high shear stress conditions, where a flow discontinuity is often detectable [3, 6]. Conclusions made from recent studies on HDPE-hydroxyapatite composites have proposed that increased pressure tends to suppress the development of wall slip, in capillary flow [16]. It is therefore clear that for multiphase polymer systems, there is no single mechanism that underpins these observations, so that the complex interactions at particle-polymer interfaces and at (or very close to) the flow boundaries must each contribute to the determination of critical conditions for wall slip. In addition, since the particle size and morphology influence the maximum packing condition and the shear viscosity, under rate-imposed conditions it follows that the developed shear stress (and by implication, wall slip behaviour) will also be dependent upon the physical characteristics of the filler, to some extent.

Therefore, the aim of the research reported is to extend existing knowledge on unfilled polymers by experimentally determining the relationships between wall slip velocity, shear stress and composition variables (filler morphology, particle size and volume fraction), using a talc-modified grade of PP that is known to exhibit a clear wall slipping response. In this way, the processing behaviour can be linked to the interaction mechanisms between the composite constituents, notably at the flow boundary. Once established, simple predictive relationships can be proposed that have potential use in flow simulation techniques for commercial polymer processes.

2. Experimental

2.1. Raw materials and filler characterisation

An extensive range of talc-filled polypropylene (PP) compositions was formulated, so that the effects of different compound variables on the wall slip behaviour could be investigated. A grade of PP homopolymer (LY6100, supplied by Montell) was used, which has a specified melt flow rate (MFR) of 4.0 dg min^{-1}, weight-average molecular weight (M_w) of 359,000 g mol^{-1} and a unimodal molecular weight distribution. Talc fillers were specifically selected in order to study separate effects of particle size (equivalent particle diameter (d_{50}) between 3.0 and 10.0 μm) and particle morphology, ranging from pseudo-spherical, to plate-like and acicular particle shape (Table I). Several suppliers were used, including Norwegian Talc (UK), Microfine Minerals (UK) and Luzenac (France). Fig. 1 shows the typical filler morphologies for the inorganic silicate materials that have different morphologies, but a similar particle size distribution. Filler particle size characteristics

TABLE I Physical properties for talc fillers

Product code	A	B	C	D	E	F
	Platelet	Acicular	Pseudo-spherical	Variable particle size		
Particle size (d_{50}, μm)[a]	4.5	4.0	4.5	3.7	5.0	10.2
Coulter counter	7.16	5.75	3.56	4.25	7.33	10.6
Malvern	8.60	6.95	5.85	7.89	9.72	17.1
BET surface area (m^2 g^{-1})	4.77	23.3	4.95	3.79	3.81	2.33
Oil absorption (cm^3/100 g)[b]	41.9	37.4	49.2	48.0	42.0	36.3
Maximum packing fraction (ϕ_{max})	0.46	0.48	0.42	0.43	0.46	0.50
Bulk density (kg m^{-3})	350	370	220	240	330	450
Density (kg m^{-3})[a]	2750	2850	2800	2780	2780	2780

[a]All data were determined experimentally with the exception of particle size (d_{50}) and density data, which were supplied by the product manufacturer.
[b]Oil absorption data were measured according to BS3483(Part B7) and are quoted as oil absorption volume (in units of cm^3) in a standard reference sample of 100 g talc filler, hence non-SI units are quoted.

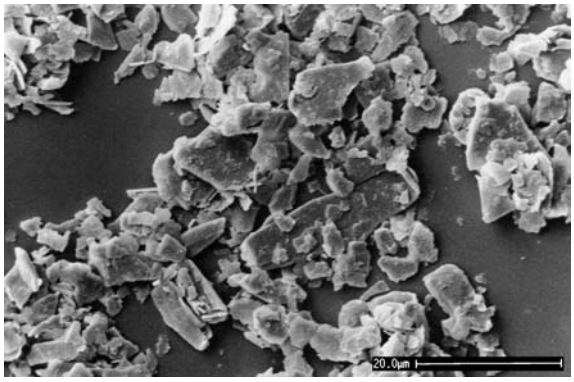

(a)

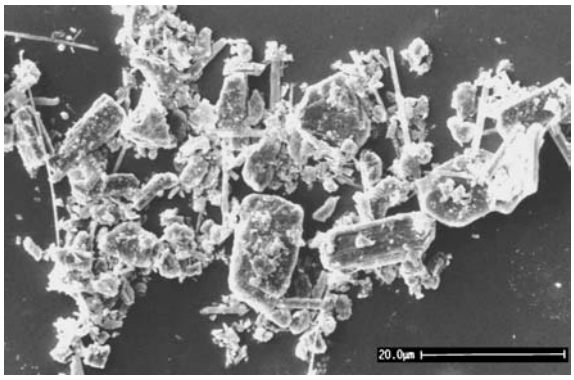

(b)

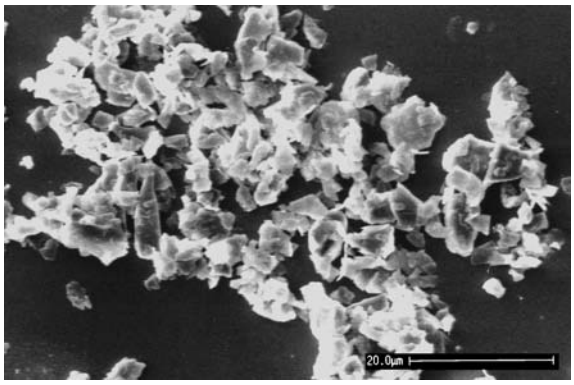

(c)

Figure 1 Scanning electron micrographs showing talc particle morphology (magnifications: × 1500) for: (a) Talc A (plate-like), (b) Talc B (acicular), (c) Talc C (pseudo-spherical).

were analysed using a Malvern Mastersizer, using laser scattering methodology. Oil absorption data were generated according to BS 3483 (Part B7, 1982) and density data have been taken directly from manufacturers' data. Table I summarises some of the important physical characteristics of the fillers used in the study.

The effects of surface modifiers, including both coating and coupling agents, were also investigated. Octyltriethoxysilane (Silquest A137, supplied by Witco) was used as a partially-reactive coating, to assist talc dispersion in PP. Chemical coupling effects were promoted using an amino-silane reagent (Silquest A1100) and also by blending with a maleic anhydride modified PP resin (Polybond 3200, supplied by Uniroyal Chemicals, UK). Particle coating with these surface treatments was achieved using a dry blending technique described elsewhere [15, 17].

2.2. Compounding and rheological methods

Filler concentration in all PP-talc composites was controlled at the compounding stage, using an APV MP2030TC twin-screw extruder (30 mm screw diameter, with 30:1 length-diameter ratio), operating with a three-stage mixing zone profile at a maximum melt temperature setting of 200°C, using a screw speed of 250 rpm. Talc fillers were dried prior to feeding and all compounds were pelletised, then dried in an air oven (80°C for 24 h) before being analysed further. Nominal concentrations of talc in the range 10–60% (by weight) were produced; actual talc concentrations were verified using an ash analysis method (according to ASTM D5630, using a muffle furnace at 800°C for one hour) and these data were used to calculate volume fractions of talc [17].

Rheological analysis of PP-talc compositions was carried out using a rate-imposed Davenport capillary rheometer operating at 200°C. Measurements were usually concentrated within a range of relatively high shear rates of relevance to high speed extrusion processes and to cavity filling effects in injection moulding. Wall slip measurements were made by performing equivalent experiments using flat-entrance dies of a constant length to diameter ratio ($L/D = 10$), but with varying capillary lengths between 8 and 20 mm. Data were analysed over a range of constant shear stress values to obtain wall slip velocity measurements according to the well-established Mooney technique. Since accuracy is critically important for carrying out this type of analysis, the pressure transducer and piston motor speed were calibrated regularly and recorded data were derived from several averaged readings, at each nominal shear rate condition. It is known that when analysing high molar mass polyolefins, there exists both primary and secondary critical shear stress levels (τ_{c1} and τ_{c2}) at which extrudate distortion (so-called sharkskin region) and gross melt fracture respectively occur. For the experiments reported in this paper, the data for wall slip refer to the onset of flow instability around (τ_{c1}).

3. Results and discussion

3.1. General shear flow behaviour—viscosity and filler characteristics

Initially, shear flow properties of the unfilled PP were analysed using capillary rheometry to produce conventional flow curves. In addition, extensional deformations were studied from experiments carried out using a zero-length, orifice die according to the Cogswell method [18, 19]. For shear flow, bilogarithmic viscosity—shear rate relationships were linear over a shear rate range of 100–2000 s^{-1} with power law index constants: $n = 0.27$ and $k = 1200$ $Ns^n m^{-2}$, for the unfilled grade of PP with weight average molecular weight (M_w of 359,000 g mol^{-1}). Compounds containing up to 60% (by weight) of talc fillers can also be characterised by a power law response, up to the point where flow instabilities occur.

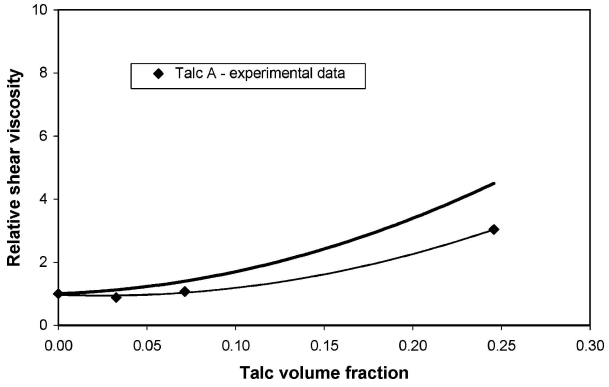

Figure 2 Normalised shear viscosity (filled/unfilled PP) versus talc filler (grade A) volume fraction (at a constant shear stress of 100 kPa). The bold trendline indicates the prediction from Equation 2, using $\phi_{max} = 0.46$, for this grade of talc.

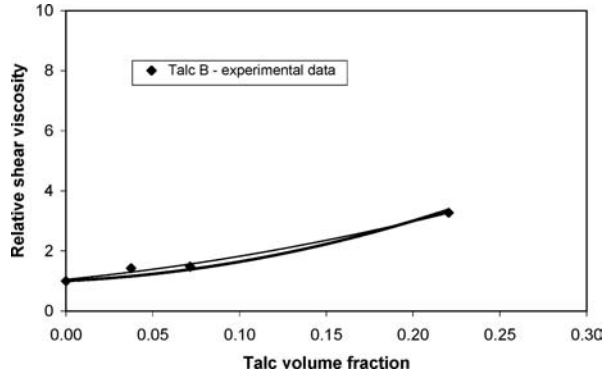

Figure 3 Normalised shear viscosity (filled/unfilled PP) versus talc filler (grade B) volume fraction (at a constant shear stress of 100 kPa). The bold trendline indicates the prediction from Equation 2, using $\phi_{max} = 0.48$, for this grade of talc.

It is therefore of interest to examine the experimental relationships between viscosity and volume fraction of talc at a constant shear stress level (Figs 2 and 3) for fillers A and B, respectively. Data on the ordinate represent relative (filled/unmodified) shear viscosity (η_r), that can also be predicted from particle volume fraction and maximum packing fraction (ϕ_{max}) data by the Maron-Pierce relationship [3, 20]:

$$\eta_r = \left[1 - \left(\frac{\phi}{\phi_{max}}\right)\right]^{-2} \quad (2)$$

ϕ_{max} is a characteristic of the particulate filler: the 'maximum packing fraction', a parameter that represents the maximum volumetric packing efficiency of the additive particles. This parameter is dependent upon particle size, morphology and surface treatment and has been determined experimentally by oil absorption data (Table I) in the research reported here. Absorption data for paraffin oil provide an indication of the packing properties of the talc filler in the non-polar, melt-state matrix of PP, whereas bulk density indicates the ability of the filler to pack when dry. Talc *C* (containing acicular particles) shows the highest oil absorption value (consistent with the lowest bulk density), indicating the effect of particle irregularity associated with this specific talc filler morphology (Fig. 1). A trend also exists between particle size and oil absorption characteristics for talc grades D-F (Table I). As the average particle size increases and assuming that a high degree of dispersion is achieved, fillers develop a broader particle size distribution that allows small particles to pack more effectively in the interstices between the more coarse particles at the other end of the distribution curve. In effect, packing efficiency is increased with particle size, as exemplified by the reduced values for oil absorption and the increase in packing fraction ϕ_{max}.

ϕ_{max} values listed in Table I have been used for viscosity prediction, using Equation 2. The extent to which the viscosity of filled polymers increases with the addition level (or volume fraction) clearly depends upon the maximum packing fraction, which is increased by particle size and is also dependent on morphology (Figs 2 and 3). It can be concluded that the level of agreement between theory and practice is reasonable, yet appears to be dependent on particle morphology, to some extent. The talc material with highest specific surface area (material B) exhibits the greatest degree of fit to the experimental data. Precise conclusions should be made with some caution however, in view of the relatively small number of data points (compounds of varying talc volume fraction) obtained by practical rheological evaluation. Surface coatings have also been shown to reduce oil absorption and increase ϕ_{max}, thereby lowering the predicted shear viscosity at a given volumetric concentration [17]. In addition, the influence of coating and coupling agents verified that at high shear rates, the behaviour of the PP compounds (even at talc concentrations up to 0.28 volume fraction) is usually dominated by the pseudoplastic response of the polymer matrix [21].

Simulations of this type would be expected to be most accurate and discriminating at relatively low shear rates approaching ideal, Newtonian conditions. In general, predicted increases in shear viscosity exceeded those derived experimentally, in view of the relatively high shear stress levels defined. It should be noted that the temperature-sensitivity of viscosity and more generalised flow behaviour has not been investigated in the present study, so that the activation energies for flow (and their dependence upon talc filler type and concentration) cannot be evaluated. However, as in the studies reported here, good agreement between theory and practical measurements has been obtained for viscosity in the high shear, pseudoplastic regime, characteristic of mixing and moulding processes, for several combinations of polymers and mineral fillers [22, 23].

3.2. Observation of wall slip in PP-talc composites

Of more direct significance to the context of the research reported here, the unfilled PP was analysed according to the multiple die methodology outlined in the experimental section, so that wall slip velocities could be analysed. Wall slip phenomena in capillary flow are well established and rheologists are generally familiar with the classical treatment of Mooney [24]. Any rheometer geometry can exhibit wall slip under appropriate circumstances, but those with high velocity

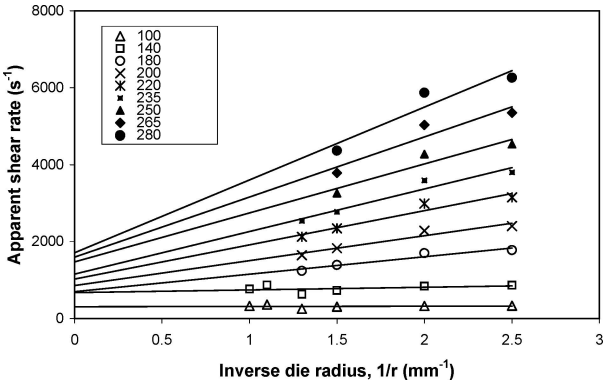

Figure 4 Wall slip analysis for unfilled PP at 200°C, obtained at various levels of shear stress (100–280 kPa, see legend).

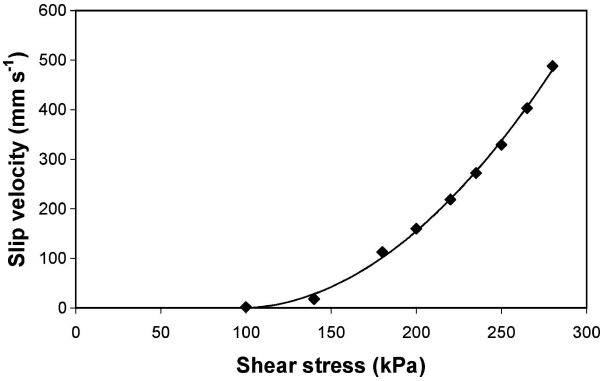

Figure 5 Wall slip velocity versus shear stress for unfilled PP at 200°C.

gradients and smooth walls at the flow boundary are most vulnerable [25], notably when processing non-polar polymers such as polyolefins.

From the standard format of shear flow curves, usually expressed as shear stress versus shear rate in bilogarithmic form, wall slip may be detectable according to the sensitivity to die geometry. Therefore, a plot of apparent shear rate versus inverse die radius can be made, over a range of shear stress levels (chosen arbitrarily from the range available) appropriate to the magnitude of shear viscosity. Fig. 4 shows a typical Mooney plot of this type for unfilled PP. According to theory [24], the magnitude of wall slip velocity is determined from the gradient of the plot; see Equation 3:

$$Q = \dot{\gamma}_T \left(\frac{\pi r^3}{4} \right) + \pi r^2 \cdot v_s \qquad (3)$$

It is clear that wall slip effects are detectable at shear stress levels exceeding 140 kPa, which represents the critical condition at which loss of adhesion to the die wall occurs. Previous work reported by Hatzikiriakos [26] analysed the wall slip response of a different type of PP and since there was no divergence of flow curves for wall shear stress below 160 kPa, it was concluded that wall slip did not occur at the test temperature of 200°C. Data for shear stresses exceeding 200 kPa were inconclusive.

In spite of the relatively simple linear regression methodology, the data in Fig. 4 are sufficiently clear to allow linear constructions to be made, in order to estimate wall slip velocity as a function of nominal wall shear stress, as shown in Fig. 5. Slip velocity increases with shear stress above a critical level at which wall adhesion first becomes unstable. For the grade of PP investigated, this critical shear stress (τ_c) is of the order of 150 kPa, with slip velocity then increasing systematically up to a maximum of around 500 mm s^{-1} at a shear stress of 270 kPa. The magnitude of the critical shear stress for PP, detected and shown in Fig. 5, is in general accordance with τ_c values published previously for linear polyolefins [9, 16, 27]. These generally lie in the range between 100 and 200 kPa and have been shown to be relatively insensitive to temperature. Beyond the critical condition, the magnitude of slip velocity can be estimated if its relationship with shear stress can be characterised. Previous work suggests that a simple power law is sufficient [5, 16, 27, 28]. Wall slip velocities of up to 450 mm s^{-1} have been determined by other researchers [9, 10, 27, 29, 30] for linear polyethylenes (LLDPE and HDPE). Empirical models that are able to describe the experimentally derived data on PP-talc from the reported research are therefore required; these are analysed and discussed further in Section 3.7.

3.3. Effect of talc volume fraction

For all PP-talc compositions, there is strong evidence that the wall slip velocity (at any given shear stress beyond the critical level) decreases when higher concentrations of talc are added. Examples of this behaviour are shown in Figs 6–7. Clearly in this case, wall slip is an inherent characteristic of the as-supplied grade of PP and is likely to be caused by the presence of low molecular weight additive species in the polymer melt [31]. The mechanism by which wall slip occurs, hence the magnitude of slip velocity, is modified by the presence of particulate talc in the melt stream. This observation is consistent with recent results reported by Ahn and White [31, 32], in which slippage effects attributed to the presence of carboxylic acid in PE were reduced when particulate additives were incorporated. The origin of slip in these composites (which did not occur in neat PE) was attributed to the incompatibility with the PE matrix and subsequent migration of the polar acid species to the die wall. Other authors have studied the influence of particulate additives and wall slip in HDPE

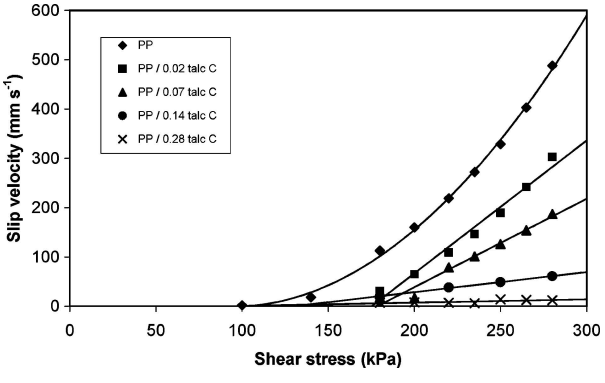

Figure 6 Slip velocity versus shear stress at 200°C for PP: effect of talc particle concentration (volume fraction 0–0.28) for talc-C.

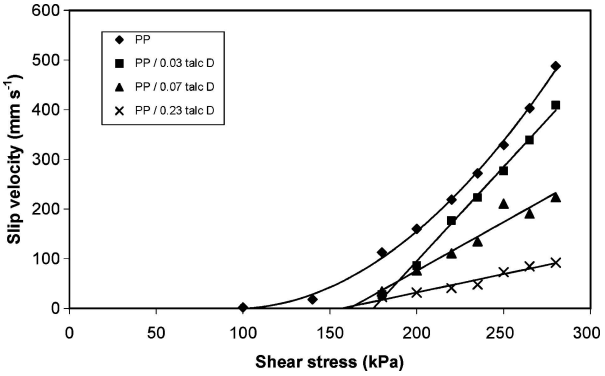

Figure 7 Slip velocity versus shear stress at 200°C for PP: effect of talc particle concentration (volume fraction 0–0.23) for talc-D.

and have interpreted results in terms of the reduced melt compressibility, when the inorganic phase is present in the polyolefin melt [16].

Qualitatively, the influence of talc volume fraction on wall slip was very similar, for all compounds analysed in the present study. Therefore, this behaviour is analysed further, with reference to other material variables (particle size, morphology and surface coating/coupling agents) in the following sections.

3.4. Effect of talc particle size and morphology

Talc is an abundant mineral used extensively in the thermoplastics compounding sector in order to enhance specific solid-state properties including modulus and creep resistance and to achieve mechanical property retention at elevated temperatures. In consequence, particle size and shape are important characteristics by which these mechanical properties are modified. It was therefore important to examine the influence of particle morphology and size distribution within the current study, in order to verify their potential influence on wall slippage characteristics of PP.

The wall slip data in Fig. 8 were generated from capillary rheometry experiments based upon PP containing nominal 10% (by weight) of talc fillers coded A, B and C. These minerals have different particle morphologies, but with a similar average particle size (see Fig. 1 and Table I). This filler concentration was chosen so that wall slip velocities were likely to be relatively high, thus increasing the potential for discriminating the respective influences of particle size and morphology. Fig. 8 shows talc particles (grade B) of highest specific surface area (Table I) generating the highest levels of wall slip, at any given shear stress. This product contains acicular particles that appear to contribute to an exceptionally high BET surface area, despite yielding similar particle size data from a range of different characterisation techniques. Whilst no data are available on the levels of particle dispersion achieved in these compounds, the presence of some high aspect ratio additives is likely to modify the flow field close to the capillary wall. Overall however, the differences are discernible yet relatively small, but at higher concentrations of talc (60% by weight; corresponding to volume fractions up to 0.31), the wall slip data were less discriminating and showed little or no effect of particle morphology.

Talc samples D-F are from the same source, but are refined to different particle size distributions, as exemplified by the data in Table I. Fig. 9 shows little influence of particle size on wall slip velocity, across the range studied, both in terms of the critical shear stress at the onset of wall slippage and also on the relationship between v_s and super-critical shear stress. Talc grade F (highest particle size) shows lower slip velocities across the shear stress range, yet this behaviour was not replicated at higher talc concentration. The observed response is likely to be due, in part, to a higher measured talc volume fraction for the PP-talc compound containing grade F (see Fig. 9, legend). An increase in slip layer thickness with increasing particle size (for aluminium/glass beads in a Newtonian polybutadiene matrix) has been reported previously [33], but the particle sizes exceeded those attributable to the talc materials used in this study.

It is clear that for the formulations studied, different talc particle morphology and particle size have only a relatively minor influence on the occurrence and development of wall slip in a non-polar melt such as PP. Since the onset of wall slippage is more closely related to small quantities of additives originally present in the polymer matrix, the investigations were therefore extended to consider the presence of surface coatings and coupling agents.

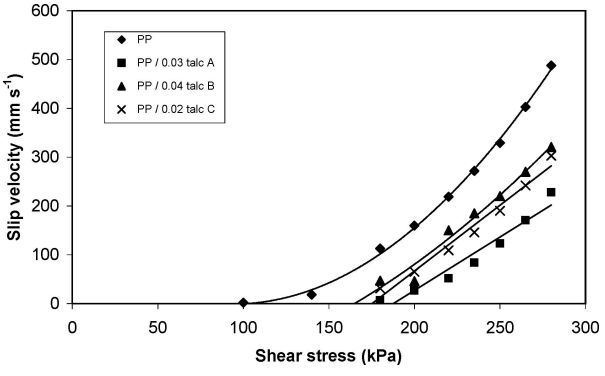

Figure 8 Slip velocity versus shear stress for PP: effect of talc particle morphology (grades A–C) at a nominal concentration of 10% by weight (see legend for actual volume fractions).

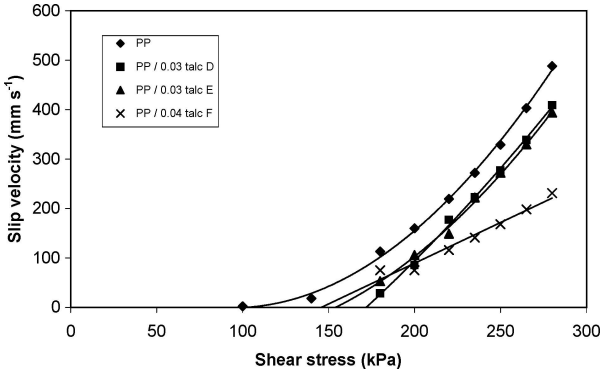

Figure 9 Slip velocity versus shear stress for PP: effect of talc particle size (grades D–F) at a nominal concentration of 10% by weight (see legend for actual volume fractions).

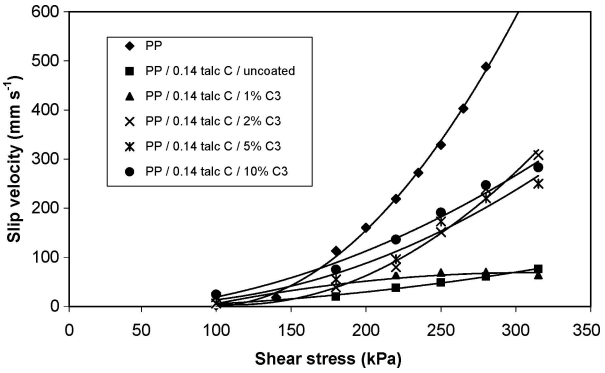

Figure 10 Slip velocity versus shear stress for PP: effect of surface modification (talc grade C volume fraction 0.14, with various concentrations of silane ester A137).

3.5. Effect of surface modification

The addition of surface modifying additives is commonplace in the reinforced thermoplastics sector, to achieve a number of key objectives, including the optimisation of both particle dispersion and polymer-particle adhesion. However, the influence of these additives on the melt flow behaviour is less well-known, so that in the research reported here, the wall slip measurements on talc-modified PP were extended to investigate the influence of both dispersion-promoting surface coatings and also chemically-reactive coupling agents. Fig. 10 shows wall slip characteristics for PP incorporating talc *C*, modified by silane A137 coating agent, within a concentration range (relative to the filler content) of between 1–10%. This coating (*n*-octyltriethoxysilane) is used in compounds such as PP-talc, in which the alkoxy end-groups bond to the inorganic filler surface and the non-polar polymer interacts physically with the coating chain. Pre-research on the filler coating process showed that additional heat is needed to initiate the reaction, which is substantially completed within 5–10 min [17].

Calculated monolayer coverage of silane coatings on talc grade C (with a specific surface area of 4.95 m^2g^{-1}—see Table I) is of the order of 1.75%, although practical data from FTIR experimentation suggested values slightly higher than this, approaching 2%. This has been confirmed in our laboratories using FTIR spectroscopy. Fig. 11 shows infrared absorption spectra of talc grade C coated with silane (2%). The absorption peak at 2928 cm^{-1}, arising from the stretching vibration of C-H bonds in the alkyl chain of the coating, can be observed when a subtraction mechanism is used to overcome the simultaneous absorption effects of the talc surface. In this way, the degree of coating can be determined for any coating conditions and Fig. 12 shows CH-absorption peak area, plotted as a function of coating concentration. Increasing peak area beyond the monolayer is not an indication of continuing reaction, but simply identifies unreacted silane in the reaction mixture.

From Fig. 10, at any shear stress exceeding 200 kPa, the compounds containing silane-coated talc are shown to have a higher slip velocity than the PP-uncoated talc compound, once the silane coating concentration exceeds 2%. The difference between the compounds is more exaggerated at higher stress levels. Two different mechanisms are likely to influence this result. First, the silane coating changes the surface chemical composition of the talc particles, producing a relatively immobile PP-rich interphase layer close to the particle surfaces. The PP-enveloped talc particles are therefore less likely to modify the boundary slip layer at the capillary wall, as the coating concentration increases. However, since the monolayer concentration of coating on talc-C particles is of the order of 2%, there will be some unreacted coating present in all compounds containing

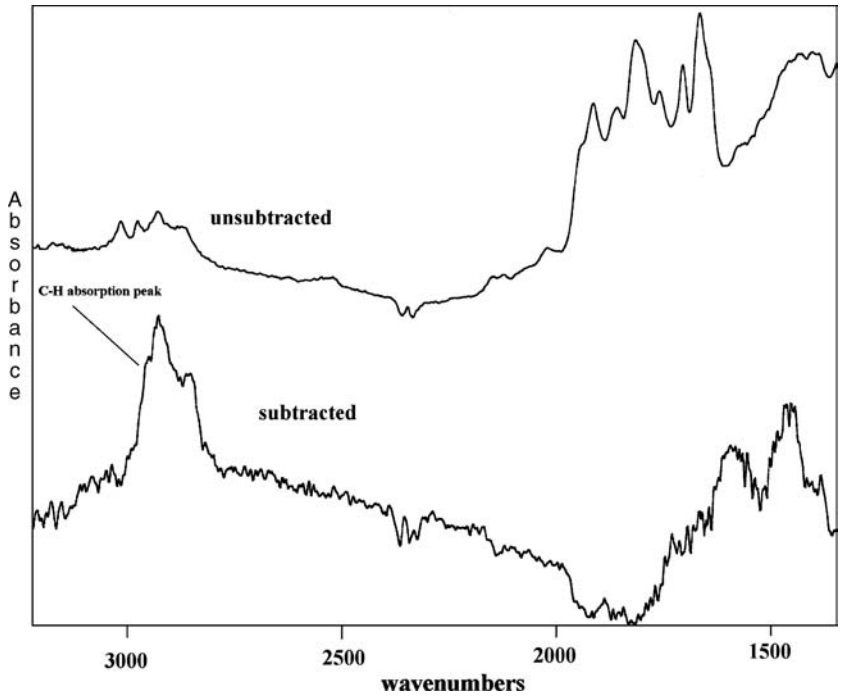

Figure 11 FTIR spectra for talc coated with 2% aminosilane C1.

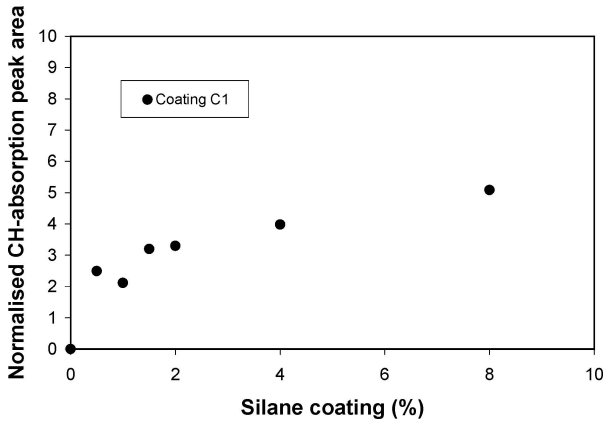

Figure 12 FTIR absorption data: effect of coating concentration (talc grade C modified by aminosilane coating C1) on the normalised peak area.

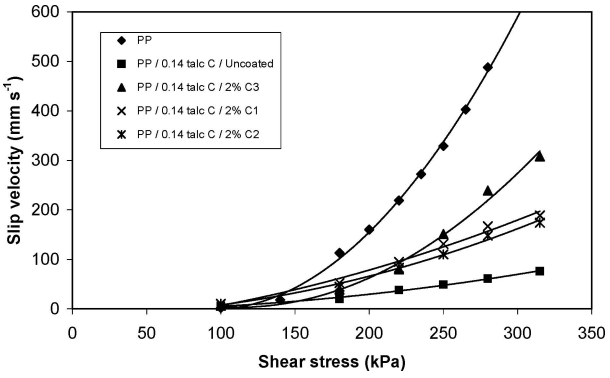

Figure 13 Slip velocity versus shear stress for PP—effect of surface modification for talc grade C (volume fraction 0.14), with a fixed concentration of various coating agents: (1) amino-silane A1100, (2) functionalised PP, (3) silane ester A137.

silane concentrations above this level. It is therefore reasonable to assume that some of this unreacted coating will migrate to the capillary boundary during dynamic flow, contributing to a more concentrated additive-rich slip layer at the boundary, resulting in further loss of adhesion under steady-state conditions. Higher stress levels allow greater transportation rates of the additive, so that slip velocity increases accordingly (Fig. 10).

This mechanism is in agreement with the suggestions made by Leblanc [34], who concluded that the addition of an external lubricant to filled elastomer compounds increases the tendency to observe wall slip, as a result of the formation of a slip-promoting additive-rich film at the flow channel boundary. Further results obtained by adding different types of surface modifying additive (Fig. 13) tend to confirm this mechanism for wall slippage. Coatings C1 and C2 promote chemical bonding, hence 'coupling' between the PP and talc particles and would therefore be expected to be less mobile within the flowing melt, once fully dispersed and reacted. Fig. 13 verifies the greater activity of modifier C3 at the flow boundary, since this coating does not react chemically with the polymer matrix and appears to have a more dominant influence on wall slip, especially at shear stress levels exceeding 250 kPa. In this research, all PP-talc compositions containing surface modifiers produced wall slip velocities higher than those observed with the uncoated compound.

3.6. Mechanism of wall slip in particle-modified polyolefins

Wall slip in unfilled PP is thought to occur as a result of the breakdown of adhesion between the bulk polymer and the flow boundary, although an alternative explanation might consider a cohesive failure in a slip layer close to the metal surface. Slippage effects in polymer melts are often reported for polyolefins, since these non-polar paraffinic polymers would be expected to show low adhesion levels with steel, in comparison to other polymers containing polar groups. If the slip mechanism can be attributed to the presence of additives, notably those that possess polar end-groups and an affinity to migrate from the bulk polymer and adhere to steel surfaces, then the slip mechanism will be dominated by the presence and activity of this molecular species [31, 32]. In this particular case, it is believed that the observation of wall slip is attributable to the presence of small concentrations of a functional, organic additive incorporated to achieve low friction surfaces in fabricated parts [35].

Short chain paraffinic species with functional end-groups are often used in this context, including so-called fatty amides such as erucamide and oleamide [36]. These additives are able to migrate from the bulk polymer and since the hydrophilic amide groups are incompatible with the non-polar PP matrix (Fig. 14), the functional groups will be aligned towards the flow boundary. In consequence, the initial (bulk) concentration of the additive required for surface modification is relatively small, so that concentrations of around 500 ppm (0.05%) are sufficient to achieve a relatively low coefficient of friction in fabricated products [36].

Even at such low concentrations, free fatty amide molecules will tend to adhere to the steel die wall during pressure-driven shear flow, creating an interphase between the bulk PP and the capillary die wall that will have a low cohesive strength, leading to the breakdown of polymer melt adhesion and the observation of wall slip. Publications that feature the direct influence of low friction, fatty amide species on polymer melt deformation behaviour at the processing stage are relatively scarce, although Ahn and White [31, 32] have recently reported the influence of low molar mass additives with aliphatic (C-18) chains, containing various polar end-groups. In this research, it is confirmed that polyolefins have relatively weak adhesion to steel die surfaces, so that migratable and incompatible polar molecules are able to replace the polymer at the flow boundary, thus demonstrating their effectiveness in creating wall slippage effects in polyolefins.

A scientific understanding of the mechanism by which transient wall slip behaviour occurs in melt state processing, as exemplified by the reported results from the reported capillary rheometry experiments, can be based upon similar principles (Fig. 14). For the unfilled PP, the short-chain amide molecules are relatively

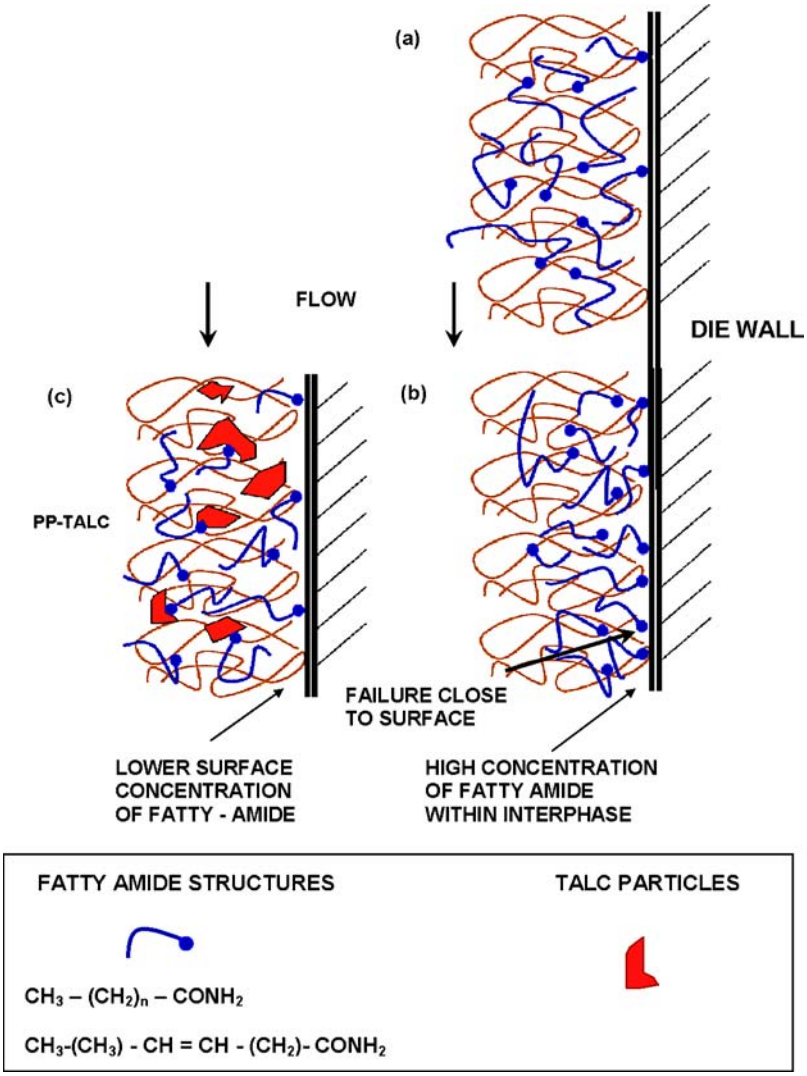

Figure 14 Schematic diagram showing the influence of talc particles on the migration of polar species to the die wall: (a) no flow—homogeneous distribution of additive; (b) dynamic flow for unfilled PP, showing surface migration of additive; (c) dynamic flow for talc-filled PP, showing reduced surface migration of polar additive.

mobile and are also incompatible with the non-polar PP matrix, so that the additive that is in direct contact with the flow boundary is more likely to adhere to the steel die surface. Surface concentration is likely to increase as flow continues and an accumulation of additive in a weak boundary layer (additive-rich interphase) is likely to occur. Therefore, it is proposed that cohesive failure occurs within this region in order to create the basis for the measured wall slip effects reported earlier in this section. Whilst the magnitude of τ_c is similar to critical stress values quoted elsewhere in the literature, it is likely that this mechanism of adhesion loss, being critically dependent upon the surface concentration of an additive with polar end-groups, accounts for the relatively high wall slip velocities that have been observed in PP.

It has been determined (Figs 6–9) that when inorganic talc filler is incorporated into the PP compounds, increasing talc concentration at or near to the flow boundary will restrict the migration rate of fatty amide molecules. The development of the weak boundary layer will therefore be delayed, even though its cohesive strength (once formed) is unlikely to be affected by the presence of the talc particles. Moreover, it is also plausible that especially at the compounding stage, the hydrophilic amide groups will promote adhesion to the silicate particles, so that the surface concentration at the die wall will be reduced. Although it is impossible to speculate as to the relative dominance of these two mechanisms, it is reasonable to assume that the latter does not completely account for the wall slip behaviour, since wall slip is still observed (albeit at reduced levels) at talc concentrations up to 60% (by weight) in PP, for which the fatty amide to talc mass ratio is relatively small (at around 0.08%).

Assuming that this slip mechanism accounts for the observed results, it is perhaps not surprising that the effects of talc particle size and morphology (described in Section 3.4) are relatively minor. Large differences in specific surface area (or particle dispersion) might influence the attraction of polar fatty amide to the talc particles, thereby reducing the tendency to observe wall slip, yet this is not substantiated by the results in Fig. 10 (effect of morphology). Finally, the wall slip data presented and discussed in Section 3.5 can also be explained by the slip mechanism presented above. Any

unreacted or non-interacting coating species can be expected to migrate into the additive-rich interphase close to the die wall and promote wall slip behaviour. This is clearly the cause of the observation in Fig. 13, showing the effect of coatings at super-monolayer level.

3.7. Empirical modelling of wall slip behaviour

Studies of wall slip in capillary flow are often based upon the treatment of Mooney [24] (Equation 3). For the PP—talc compositions investigated, slip velocities were calculated accordingly, then re-plotted as a function of shear stress, to obtain the raw data that have been presented earlier in the paper (Figs 5–10 and 13).

Model 1: Linear relationship beyond critical shear stress (τ_c)

For situations where the subsequent response between slip velocity (v_s) and shear stress (τ) appears to be linear beyond the critical shear stress at which wall slip is initiated (τ_c) (e.g. Figs 6–7), the behaviour can be modelled according to a simple empirical relationship (Equation 4).

$$v_s = \left(\frac{\tau - \tau_c}{k_1(\phi)}\right) \tag{4}$$

k_1 is a slip coefficient that is dependent upon the volume fraction (ϕ) of particulate additive; its magnitude is a measure of the sensitivity of wall slip velocity to shear stress, beyond τ_c.

This analysis is able to generate a single-point value for τ_c and has been applied to PP-talc composites based upon all six grades of talc detailed in Table I, at filler concentrations up to 60% (by weight). Overall, values of τ_c are similar for all talc-filled PP compounds investigated (Table II). In contrast, the slip coefficient k_1 demonstrates significant differences in the sensitivity of slip velocity to shear stress, for each set of talc-filled PP compounds. As the volume fraction of talc increases, the dependence of slip velocity on shear stress decreases and also, the maximum observed slip velocity also reduces at higher filler concentration. For the unfilled PP polymer however, k_1 has not been reported since the relationships between slip velocity and shear stress were clearly non-linear (Fig. 5). Overall therefore, whilst this type of empirical relationship is useful to estimate τ_c, an improved model is required to simulate the wall slip behaviour in a manner that describes all PP-talc compositions analysed.

TABLE II Parameters for critical shear stress and slip coefficient for PP – Talc composites—Effect of particle morphology

Compounds (Volume fraction talc, ϕ)	Talc particle attributes	Critical shear stress, τ_c (kPa)	Slip coefficient (k_1)
PP–Talc A (0.03)	Plate-like	190	2.21
(0.07)	$d_{50} = 4.5\ \mu$m	164	3.82
(0.25)		124	0[a]
PP–Talc B (0.04)	Acicular	174	2.74
(0.07)	$d_{50} = 4.0\ \mu$m	159	1.60
(0.22)		217	0[a]
PP–Talc C (0.02)	Pseudo-	177	2.72
(0.07)	spherical	180	1.69
(0.28)	$d_{50} = 4.5\ \mu$m	163	0.07
PP–Talc D (0.03)	Pseudo-	175	3.81
(0.07)	spherical	165	1.90
(0.23)	$d_{50} = 3.7\ \mu$m	161	0.69

[a]Zero values of gradient (k_1) taken from individual data points imply that slip velocities were very low and were insensitive to shear stress, over the range studied.

Model 2: Power Law relationship between v_s and τ_w

Previous reported work on wall slip phenomena [8, 10, 27, 28, 30] in polymer melts has demonstrated the use of a simple power law to describe the relationship between wall slip velocity (v_s) and super-critical wall shear stress (τ_w):

$$v_s = A \cdot \tau_w^m \tag{5}$$

Therefore:

$$\log v_s = \log A + m \cdot \log \tau_w \tag{6}$$

Typical values of wall slip power law constants for HDPE and LLDPE were quoted as follows, depending upon temperature and resin molecular structure [8]:

$$\text{Log}A = 0.2 - 6.9 \text{ and } m = 1.7 - 3.2$$

(Parameter A is in units of $(\text{MPa})^{-m} \cdot \text{ms}^{-1}$)

Using a similar approach, further analysis of the raw data from which Figs 6–7 (for example) were compiled has been used to generate Figs 15–17, in bilogarithmic, power law format. The degree of linearity is generally good (correlation coefficients between 0.92 and 0.99) and the effect of filler content is very clear, with a reduction in wall slip velocity (at any given wall shear stress), but little effect on the exponent (m). Values of constants A and m are quantitatively similar to those reported in the literature [8, 28]. It can be seen in Figs 15–16 that the very low wall slip velocities observed in compounds containing the highest volume fractions of talc filler

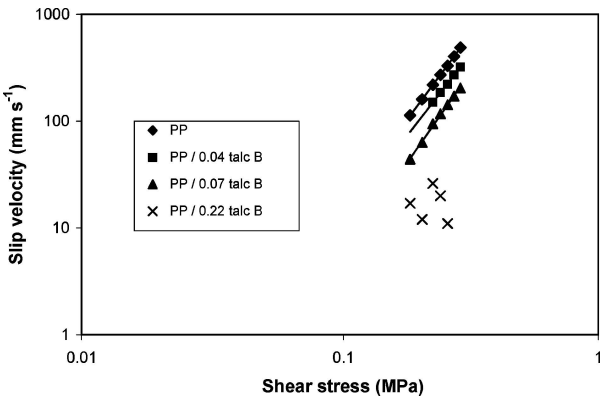

Figure 15 Power law analysis for wall slip velocity—shear stress relationships: PP/various concentrations of talc (see legend—volume fractions of talc grade B).

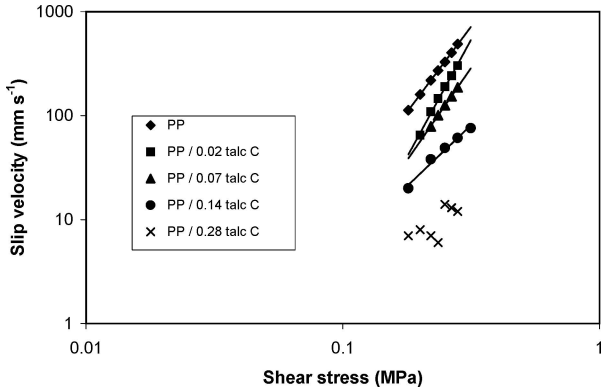

Figure 16 Power law analysis for wall slip velocity—shear stress relationships: PP/various concentrations of talc (see legend—volume fractions of talc grade C).

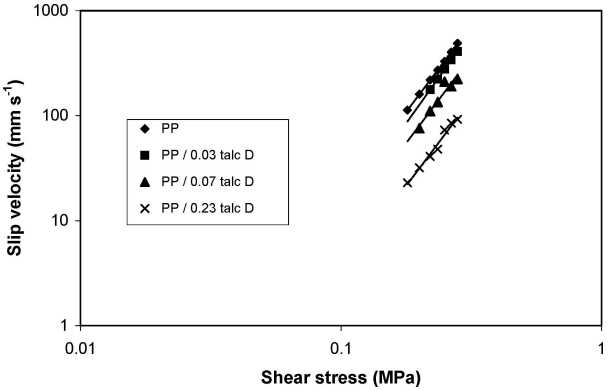

Figure 17 Power law analysis for wall slip velocity—shear stress relationships: PP/various concentrations of talc (see legend—volume fractions of talc grade D).

(hence high variation of data points) leads to excessive scatter at these high concentrations. Although the data for only talc materials B, C and D are presented here, qualitatively similar responses were obtained for other grades. Quantitative values of intercept (A) and power law exponent (m) have therefore been computed for all compounds (PP+talc fillers A-F) and these are listed in Tables III–IV, showing the effects of talc morphology and particle size, respectively.

TABLE III Parameters for the power law slip velocity model: PP compounded with Talc–Effect of particle morphology

Compound (filler volume fraction, ϕ)	A (MPa)$^{-m}$ ·mm s^{-1}	Log A	m	v_s (mm s^{-1})
PP Unfilled	31,900	4.50	3.3	334
PP/Talc A – platelet				
0.03	824,000	5.92	6.4	117
0.07	107,000	5.03	4.2	317
0.25	[a]			24
PP/Talc B – acicular				
0.04	17,500	4.24	3.1	225
0.07	18,000	4.26	3.5	141
0.28	[a]			11
PP/Talc C – pseudo-spherical				
0.02	99,100	4.50	4.5	188
0.07	17,400	4.24	3.6	125
0.14	1,200	3.09	2.4	47
0.23	[a]			14

[a]Correlation coefficient was less than 0.98, so that experimental data have been quoted in the relevant rows of the table.

TABLE IV Parameters for the power law slip velocity model: PP compounded with Talc–Effect of particle size

Compound (filler volume fraction, ϕ)	A (MPa)$^{-m}$ ·mm s^{-1}	Log A	m	v_s (mm s^{-1})
PP Unfilled	31,900	4.50	3.3	334
PP/Talc D ($d_{50} = 3.7\mu$m)				
0.03	34,000	4.53	3.5	277
0.07	16,300	4.21	3.3	169
0.23	6,470	3.81	3.3	66
PP/Talc E ($d_{50} = 5.0\mu$m)				
0.03	129,000	5.11	4.5	263
0.07	[a]			27
0.21	[a]			109
PP/Talc F ($d_{50} = 10.2\mu$m)				
0.04	5,890	3.77	2.6	169
0.07	37,200	4.57	3.7	214
0.31	[a]			

[a]Correlation coefficient was less than 0.98, so that experimental data have been quoted in the relevant rows of the table.

Parameters for the power law model have therefore been computed from the experimental data. In addition, the wall slip values at an arbitrary level of wall shear stress relevant to commercial processes ($\tau = 250$ kPa) have been calculated from the power law. In instances where the correlation coefficient (for plots of log v_s versus log τ) was relatively low (below 0.98), the data are identified in Tables III–IV and the wall slip values quoted in the final column were those measured experimentally. Predicted relationships between slip velocity and talc filler content are expressed in Fig. 18 and show clearly the reduction in wall slip velocity that is predicted when talc is incorporated into the non-polar PP matrix in increasing quantities. From these data, it is deduced that the respective influence of both filler particle size and morphology is marginal, relative to the dominant effects of filler concentration.

If v_s can be predicted using either of these empirical models, there is obvious potential to incorporate such an algorithm into the slip velocity term in Equation 3, in order to account for the effects of wall slip in polymer processing computational analysis. It has already been established that the occurrence of wall slip compromises the accuracy of flow simulation in extrusion processes [5, 37]. Flow analysis and viscosity data may then be corrected, or modified to take account of wall slipping compounds, such that the accuracy of flow analysis procedures might be enhanced.

In view of the relatively high levels of correlation and the qualitative agreement with similar data derived from other polyolefins [8, 28], it is proposed that this analysis provides a basis from which wall slip characteristics of filled polymers might be predicted and used in subsequent computational process modelling. The work reported has extended existing knowledge by analysing the influence of material composition (particulate filler concentration) on the power law parameters for wall slip effects in PP, using a mechanism based upon the interaction between migrating polar additives and the die wall.

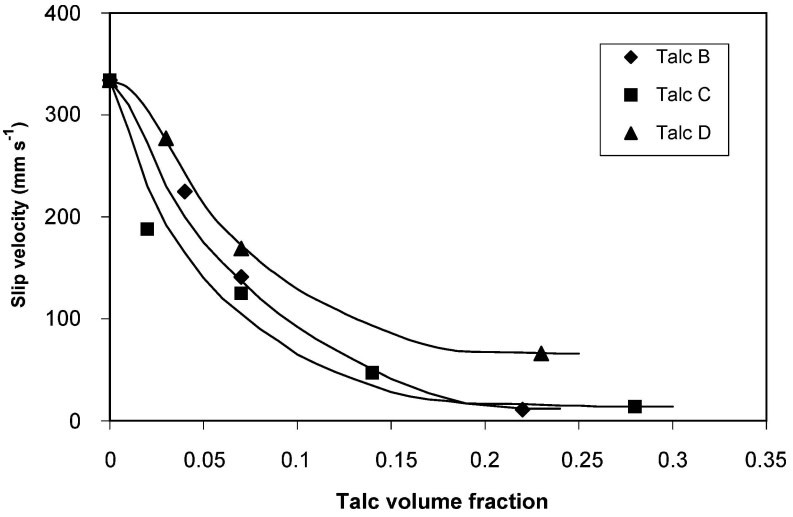

Figure 18 Wall slip velocity (at an arbitrary shear stress of 250 kPa) predicted from the power law parameters (A and m), plotted against talc volume fraction in PP (materials B, C, D).

4. Conclusions

The general shear flow behaviour of PP-talc composites in capillary dies at relatively high shear rates is dominated by the pseudoplastic nature of the matrix polymer. The Maron-Pierce relationship has been used successfully to model the dependence of shear viscosity (at a constant stress) on talc volume fraction, using particle packing data. Packing fraction (ϕ_{max}) is a function of talc morphology, particle size and surface coating concentration.

However, the dependence of shear flow behaviour on die geometry has demonstrated the occurrence of wall slip in an unfilled grade of PP. Beyond the critical shear stress (τ_c), wall slip velocity increases with stress but to an extent dependent upon the volume fraction of talc filler, with slip velocity (at any given stress) decreasing with talc filler concentration. At a relatively low volume fraction ($\phi = 0.03$), an acicular grade of talc with high specific surface area exhibited the highest wall slip velocity, yet at higher concentrations, the wall slip data were less discriminating and showed little sensitivity to the effects of particle morphology. The presence of organo-silane coatings on the talc particles modifies wall slip relative to compounds containing uncoated filler, once the coating concentration exceeds the monolayer coverage. Unreacted coating is likely to migrate to the die wall boundary during dynamic flow, notably at high stress levels, thereby reducing the cohesive strength of the interlayer and increasing wall slip velocity. A mechanism has been proposed to account for these observations, based upon the surface activity of short-chain, amide molecules and the development of an additive-rich interphase at the die wall, which has low cohesive strength and subsequently controls the wall slippage effects in PP-talc composites.

Relationships between wall slip velocity and shear stress have been modelled in order to form predictive relationships between these variables. A linear relationship between v_s and shear stress allows the critical stress (τ_c) and a slip coefficient (k_1) to be defined; the latter coefficient is more sensitive to PP-talc formulation than τ_c. Models published previously have been based upon a power law relationship, that has been shown to be adequate in describing the dependence of v_s on shear stress, in this study. The results from this research have extended this approach by accounting for the sensitivity of v_s to particle volume fraction (ϕ), exemplified by the presence of talc particles of varying particle size and morphology.

The observed behaviour has been attributed to a mechanism by which short-chain, relatively mobile additives containing polar end-groups are able to migrate to the flow boundary at the die wall. Slip effects are evident in PP above a critical shear stress of around 150 kPa, at which cohesive failure is likely to occur within an additive-rich interphase, which exists very close to the flow boundary. Interactions between the short-chain polar additives, talc particles and surface coatings, notably at the flow boundary and at polymer-particle interfaces, are complex. However, this research demonstrates that there is scope to systematically control the additive concentrations in order to optimise flow behaviour and the subsequent physical properties of artefacts manufactured from polymer-particle composites.

Acknowledgements

The Association of Commonwealth Universities (ACU) is acknowledged for the award of a Research Scholarship for Dr. Khan.

References

1. H. S. KATZ and J. V. MILEWSKI, "Handbook of Fillers for Plastics," 2nd ed. (Longman, 1995).
2. R. N. ROTHON (ed.), "Particulate Filled Polymer Composites," (Longman, 1995).
3. R. JOSEPH, M. T. MARTYN, K. E. TANNER, P. D. COATES and W. BONFIELD, *Plast. Rubb. & Composites* **30** (2001) 197.
4. J. A. BRYDSON, "*Flow Properties of Polymer Melts*," 2nd ed., (Godwin, 1981).
5. R. A. WORTH, J. PARNABY and H. A. A. HELMY, *Polym. Eng. Sci.* **17** (1977) 257.
6. H. POTENTE, M. KURTE and H. RIDDER, *Intern. Polym. Proc.* **XVIII** (2003) 115.

7. H. POTENTE and H. RIDDER, Presented at PPS-17 Intnl. Conf., Paper 085, pp. 1–17, Montreal, Canada, (2001).
8. H. J. LARRAZABAL and A. N. HRYMAK, *Intern. Polym. Proc*. **XVII** (2002) 44.
9. A. RAMAMURTHY, *J. Rheol*. **30** (1986) 337.
10. S. G. HATZIKIRIAKOS, C. W. STEWART and J. M. DEALY, *Intern. Polym. Proc*. **VIII** (1993) 30.
11. S. G. HATZIKIRIAKOS and J. M. DEALY, *Intern. Polym. Proc*., **VIII** (1993) 36.
12. G. MENNING, *Kunststoffe* **74** (1984) 296.
13. D. A. HILL, T. HASEGAWA and M. M. DENN, *J. Rheol*. **34** (1990) 891.
14. B. HAWORTH and C. L. RAYMOND, BPF/MOFFIS Intnl. Conf. *'Eurofillers 97'*, Manchester 1997, p. 251.
15. B. HAWORTH, C. L. RAYMOND and I. SUTHERLAND, *Polym. Eng. Sci*. **40** (2000) 1953.
16. R. JOSEPH, M. T. MARTYN, K. E. TANNER, P. D. COATES and W. BONFIELD, Plast., *Rubb. & Composites* **30** (2001) 205.
17. S. W. KHAN, PhD Thesis, Loughborough University, 2001.
18. F. N. COGSWELL, *Polym. Eng. Sci*. **12** (1972) 64.
19. F. N. COGSWELL, *Polymer Melt Rheology*, 2nd ed., (Woodhead Press, 1994).
20. Y. BOMAL and P. GODARD, *Polym. Eng. Sci*. **36** (1996) 237.
21. M. S. BOAIRA and C. E. CHAFFEY, *Polym. Eng. Sci*. **17** (1977) 715.
22. B. HAWORTH and S. JUMPA, Plast. *Rubb. & Comp.* **28** (1999) 363.
23. B. HAWORTH and I. SUTHERLAND, Presented at PPS-17 Intnl. Conf., Paper 277, (Montreal, Canada, May 2001), p. 1.
24. M. MOONEY, *J. Rheol*. **2** (1931) 210.
25. H. A. BARNES, *J. Non-Newt. Fluid Mech.* **56** (1995) 221.
26. I. B. KAZATCHCHKOV, S. G. HATZIKIRIAKOS and C. W. STEWART, *Polym. Eng. Sci*. **35** (1995) 1864.
27. S. G. HATZIKIRIAKOS and J. M. DEALY, *J. Rheol*. **36** (1992) 703.
28. Anon, 'Flow-2000' Polymer Rheology & Software, Compuplast International Inc.
29. L. L. BLYLER and A. C. HART, *Polym. Eng. Sci*. **10**(4) (1970) 193.
30. D. S. KALIKA and M. M. DENN, *J. Rheol*. **31** (1987) 815.
31. S. AHN and J. L. WHITE, *Intern. Polym. Proc*. **XVIII** (2003) 243.
32. S. AHN and J. L. WHITE, *Intern. Polym. Proc*., **XIX** (2004) 21.
33. F. SOLTANI and U. YILMAZER, *J. Appl. Polym. Sci*. **70** (1998) 515.
34. J. L. LEBLANC, J. P. VILLEMAIRE, B. VERGNES and J. F. AGASSANT, *Plast. Rubb. Proc. Appl.* **11** (1989) 53.
35. C. MAIER, "Polypropylene: The Definitive User's Guide and Databook, Plastic Design Library, (New York, 1998).
36. N. ROHSE, P. DEWAEL and I. VAN DE MEEREN, "Presented at VDI Int. Conf., VDI, Bad Homburg, Germany, September 1999.
37. H. HIGUCHI and K. KOYAMA, *Intern. Polym. Proc*. **XVIII** (2003) 349.

Received 15 January
and accepted 2 February 2005